Title

Acetone in the atmosphere of Hong Kong: Abundance, sources and photochemical precursors

Permalink

https://escholarship.org/uc/item/7536z3t6

Authors

Guo, H
Ling, ZH
Cheung, K
et al.

Peer reviewed
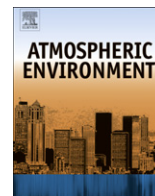
Acetone in the atmosphere of Hong Kong: Abundance, sources and photochemical precursors

H. Guo [a,*], Z.H. Ling [a], K. Cheung [a], D.W. Wang [a], I.J. Simpson [b], D.R. Blake [b]

[a] *Air Quality Studies, Department of Civil and Environmental Engineering, The Hong Kong Polytechnic University, Hong Kong*
[b] *Department of Chemistry, University of California, Irvine, CA, USA*

HIGHLIGHTS

► Ambient acetone was mainly caused by vehicular emission and secondary formation in Hong Kong.
► *i*-Butene was the main precursor of secondary acetone at the mountain site.
► Oxidation of *i*-butane was the major source of secondary acetone at the urban site.

ARTICLE INFO

ABSTRACT

Intensive field measurements were carried out at a mountain site and an urban site at the foot of the mountain from September to November 2010 in Hong Kong. Acetone was monitored using both canister air samples and 2,4-dinitrophenylhydrazine cartridges. The spatiotemporal patterns of acetone showed no difference between the two sites ($p > 0.05$), and the mean acetone mixing ratios on O_3 episode days were higher than those on non-O_3 episode days at both sites ($p < 0.05$). The source contributions to ambient acetone at both sites were estimated using a receptor model i.e. Positive Matrix Factorization (PMF). The PMF results showed that vehicular emission and secondary formation made the most important contribution to ambient acetone, followed by the solvent use at both sites. However, the contribution of biogenic emission at the mountain site was significantly higher than that at the urban site, whereas biomass burning made more remarkable contribution at the urban site than that at the mountain site. The mechanism of oxidation formation of acetone was investigated using a photochemical box model. The results indicated that *i*-butene was the main precursor of secondary acetone at the mountain site, while the oxidation of *i*-butane was the major source of secondary acetone at the urban site.

© 2012 Elsevier Ltd. All rights reserved.

1. Introduction

Acetone is an abundant carbonyl compound in the atmosphere. It exerts a substantial effect on atmospheric oxidative capacity. Apportioning acetone sources is complicated as acetone is emitted into the atmosphere from both natural and anthropogenic sources. Natural sources include direct emissions from vegetation, decaying organic material and secondary production by the oxidation of biogenic hydrocarbons (Singh et al., 1994; Jacob et al., 2002). Anthropogenic sources are vehicular emissions, solvent use and secondary production by the oxidation of man-made hydrocarbons (Singh et al., 1994; Jacob et al., 2002). In addition, biomass burning is found to emit acetone (Singh et al., 1994), whereas the role of the ocean was considered for the first time by de Laat et al. (2001) and

Jacob et al. (2002). de Reus et al. (2003) further speculated the release of acetone from the ocean in relatively clean regions and the uptake of acetone by the ocean in more polluted areas. However, Singh et al. (2004), Williams et al. (2004), Taddei et al. (2009) and Fischer et al. (2012) concluded that the ocean is globally a net sink for acetone.

It is well known that acetone is a source of NO_x, peroxy, alkoxy radicals and peroxyacetylnitrate (PAN) in the free troposphere due to photolysis, suggesting its significant importance in tropospheric chemistry (e.g. Singh et al., 1994; Arnold et al., 1997; Floberth et al., 2006). Acetone in the atmosphere is removed mainly by photolysis and reaction with OH radical, resulting in a mean lifetime for acetone of about 15 days (Gierczak et al., 1998; de Laat et al., 2001). In addition, deposition to land and oceans has been reported by Singh et al. (1994) and Jacob et al. (2002).

Many studies have been carried out on the measurements of atmospheric acetone concentrations in the past two decades at

surface sites (e.g. Solberg et al., 1996; Slemr et al., 1996; Goldstein and Schade, 2000; Guo et al., 2004; Wang et al., 2005; Feng et al., 2005; Rubio et al., 2006; Mao et al., 2006; Huang et al., 2008), at mountain sites (e.g. Legreid et al., 2008; Chi et al., 2008), and during aircraft campaigns (e.g. Singh et al., 1994; de Laat et al., 2001; de Reus et al., 2003; Eerdekens et al., 2009; Sprung and Zahn, 2010; Lai et al., 2011; Elias et al., 2011). However, very limited studies have been done in subtropical Hong Kong and all of them only reported the abundance of acetone (e.g. Ho et al., 2002; Guo et al., 2004). Some key scientific issues such as the sources of acetone and their contributions to acetone, and major hydrocarbons responsible for photochemical acetone formation, are poorly understood.

Hong Kong has been facing the challenge of air pollution problems since 1980s, due to highly dense population and rapid economic growth. Previous investigations demonstrate that main carbonyl emission sources in urban Hong Kong are vehicular and industrial emissions (Ho et al., 2002; Guo et al., 2004). Owing to its unique topography and meteorological conditions, the South China coast is under the influence of Asian monsoon circulation. Polluted urban plumes in Hong Kong can be brought to the South China Sea and further downwind regions in autumn and winter. Thus, the acetone emissions in Hong Kong could have profound impact on the oxidative capacity of marine boundary layer over the South China Sea and western Pacific. Hence, this study will investigate the spatiotemporal variations of atmospheric acetone, quantify source contributions to ambient acetone using a receptor model, and reveal major mechanisms of photochemically formed acetone with a photochemical box model.

2. Methodology

2.1. Description of sampling sites

Hong Kong (22°60′–22°36′N, 113°48′–114°30′E), situated on the coast of South China, is enclosed by the Pearl River Delta (PRD) region and has a total area of 1104 km^2 and a population of seven million people (HKCSD, 2010). The climate in Hong Kong is dominated by the Asian monsoons. Each year can be divided into two distinct wet and dry seasons. The wet season lasts from April to September when the summer monsoon prevails. During this time the prevailing wind is from the southeast, south and southwest, and it is hot, humid and rainy. The dry season lasts from October to March when the Asian winter monsoon is dominant and the prevailing wind is from the northeast and north.

In this study, field measurements were simultaneously carried out at different elevations on the highest mountain in Hong Kong, Mt. Tai Mo Shan (TMS), from 06 September to 29 November, 2010 (Fig. 1). The Hong Kong Environmental Protection Department (HKEPD) air quality monitoring station at Tsuen Wan (TW) was selected as the measurement site at the foot of the mountain (22.373°N, 114.112°E, elevation of 10 m). TW is a mixed residential, commercial and light industrial area in the New Territories in Hong Kong. The monitoring site was located on the rooftop of a building approximately 15−20 m above the ground level, which is adjacent to a main traffic road and surrounded by residential and industrial blocks. The high-elevation site was set up on the rooftop of a building on TMS (22.405°N, 114.118°E) at an elevation of 640 m. Because of its unique topography, mountain-valley breezes and sea-land breezes are often observed at TMS. These mesoscale circulations enhance the interaction of polluted urban air and the mountain air. The TW and TMS sites are separated by a distance of 7 km and an elevation of 630 m. Detailed description on the TMS site can be found in Guo et al. (2012).

2.2. Measurement techniques

2.2.1. Continuous measurements of O_3, CO, SO_2 and NO

At TW, O_3, CO, SO_2, $NO−NO_2−NO_x$ and meteorological parameters were measured at the HKEPD monitoring station using similar instruments and quality assurance and control protocols to those in the US air quality monitoring program (http://epic.epd.gov.hk/ca/uid/airdata). At TMS, measurement instruments were installed in a room of a building and ambient air samples were drawn through a 5 m long perfluoroalkoxy (PFA) Teflon tube (OD: 12.7 mm; ID: 9.6 mm). The inlet of the sampling tube was located 2 m above the rooftop of the building and was connected to a PFA manifold with a bypass pump drawing air at a rate of 5 L min^{-1} into the intakes of the analyzers for O_3, CO, SO_2 and $NO−NO_2−NO_x$. Meteorological parameters were monitored by an integrated sensor suite. For details on the analyzers and calibration, please refer to Guo et al. (2012).

2.2.2. Sampling and analysis of carbonyls

Carbonyl samples were collected on selected non-O_3 episode (i.e. 28 September, 02, 08, 14, 18−19, 27−28 October, and 20−21 November) and O_3 episode days (i.e. 23−24, 29−31 October, 01−03, 09 and 19 November) at both sites. The potentially high O_3 episode days were selected based on weather prediction and

Fig. 1. The sampling sites and the surrounding environment.

meteorological data analysis, and were usually related to stronger solar radiation, weaker wind speeds, and less vertical dilution of air pollution compared to non-O₃ episode days. Silica cartridges impregnated with acidified 2,4-dinitrophenylhydrazine (DNPH) were used for sampling. During non-O₃ episode days, carbonyl samples were simultaneously collected from 7 a.m. to 9 p.m. every 2 h at both sites. For O₃ episode days, carbonyls were consecutively collected every 2 h from 7 a.m. to 9 p.m., with additional samples collected at midnight and 3 a.m. Totally 164 and 165 valid carbonyl samples were collected during O₃ and non-O₃ episode days, respectively. It is noteworthy that some samples were not collected as originally scheduled and/or were discarded due to logistical difficulty and failure of sampling.

All cartridges were stored in a refrigerator at 4 °C after sampling. The sampled carbonyl cartridges were eluted with acetonitrile and analyzed by the high performance liquid chromatography (HPLC) system through an auto-sampler. The operating conditions of the HPLC are shown in Table 1. Typically, C_1–C_6 carbonyl compounds can be measured effectively by this technique with a detection limit of ∼0.2 ppbv.

The carbonyls were calibrated using five standard concentrations spanning the concentrations of interest for ambient air. Good linear relationships were found between the concentrations and responses for all identified carbonyls ($R^2 > 0.998$). Cartridge collection efficiency was determined with two cartridges in series; over 98% carbonyl compounds were found in the first cartridge. Relative percent differences for duplicate analysis were within 10%.

For comparison, ambient non-methane hydrocarbon (NMHC) and oxygenated hydrocarbon samples were collected using cleaned and evacuated 2-L electro-polished stainless steel canisters. The canisters were prepared and delivered to Hong Kong by the Rowland/Blake group at University of California, Irvine (UC-Irvine). A flow-controlling device was used to collect 1-h integrated samples. During non-O₃ episode days, hourly samples were collected from 7 a.m. to 7 p.m. (one sample every 2 h) per day at both sites. For O₃ episode days, hourly samples were consecutively collected from 9 a.m. to 4 p.m. with additional samples collected at 6 p.m., 9 p.m., midnight, 3 a.m. and 7 a.m. Totally, 201 and 183 VOC samples were collected at TMS and TW, respectively.

The NMHC samples were returned to the laboratory at UC-Irvine for chemical analysis. The analytical system, which is fully described in Simpson et al. (2010), uses multicolumn gas chromatography (GC) with five column-detector combinations that optimize the detection of more than 70 speciated NMHCs and some carbonyl compounds including acetone. The oven parameters employed for each GC can be found in Colman et al. (2001). Generally, alkanes, alkenes and aromatics have a detection limit of 3 pptv, a precision of 3%, and an accuracy of 5%. The detection limit for acetone is 100 pptv; the precision is 30% and the accuracy is 30%.

Correlation between acetone data obtained from HPLC and GC–MS analysis showed a slope of 0.93 ($R^2 = 0.68$), suggesting that the methods used in this study were reliable for acetone analysis (Fig. 2).
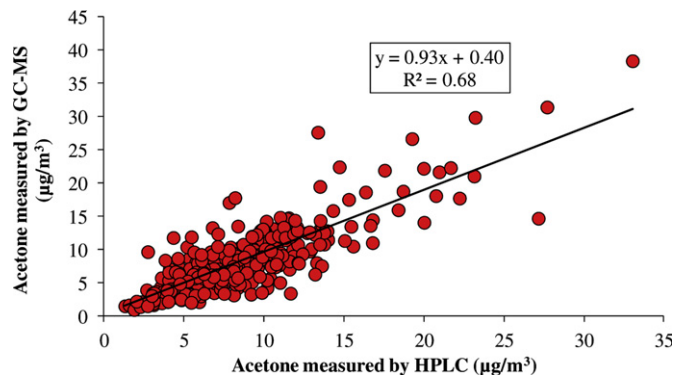

Fig. 2. Comparison of acetone concentration analyzed by HPLC and by GC–MS.

2.3. Model simulation

2.3.1. PMF receptor model

PMF was used to resolve the acetone data obtained at TMS and TW. Briefly, a mass balance equation can be written to account for all m chemical species in the n samples as concentrations from p independent sources:

$$x_{ij} = \sum_{k=1}^{p} g_{ik}f_{kj} + e_{ij}, \tag{1}$$

where x_{ij} is the jth species concentration measured in the ith sample, g_{ik} is the species contribution of the kth source to the ith sample, f_{kj} is the jth species fraction from the kth source, e_{ij} is residual associated with the jth species concentration measured in the ith sample, and p is the total number of independent sources (Paatero, 1997). PMF provides a matrix of the source profiles and a matrix of the time series of source contributions without prior knowledge of NMHC and carbonyl sources. In PMF, sources are constrained to have non-negative species values, and no sample can have a negative source contribution.

To solve the PMF problem, an object function to be minimized is introduced:

$$Q(E) = \sum_{i=1}^{m} \sum_{j=1}^{n} \left[\frac{e_{ij}}{s_{ij}}\right]^2, \tag{2}$$

where s_{ij} is an uncertainty estimate in a data point with the jth species measured in the ith sample. PMF uses a unique algorithm in which both source profile and contribution matrices are varied simultaneously in each least squares step (Paatero, 1997).

2.3.2. Photochemical box model

The box model simulates complex chemical reactions within a well mixed boundary layer air parcel, which extends from the Earth's surface up to the top of a diurnally varying boundary layer. The boundary layer height is made to vary from 300 m at night to a maximum of 1200 m during the daytime. The chemical mechanism employed in the photochemical box model is an extended version of the MCMv3.1, which is a near-explicit chemical mechanism describing the detailed degradation of a large number of emitted organic compounds and the resulting generation of O₃ and other secondary pollutants under conditions appropriate to the atmospheric boundary layer (Jenkin et al., 1997). It currently describes the oxidation of methane and 139 non-methane VOCs, and contains around 13,500 reactions involving 5900 chemical

Table 1
Gradient separation of C_1–C_7 aldehyde and ketone derivatives.

Column	Nava-Pak C18 3.9 × 150 mm
Mobile phase	A: water/acetonitrile/tetrahydrofuran 60/30/10
Gradient	B: water/acetonitrile 40/60
Flow rate	100% A for 2 min then a linear gradient from 100% A to 100% B in 18 min, 100% B for 4 min
Injection volume	20 μL
Detection	Absorbance at 360 nm

species. The MCM can be accessed via the University of Leeds website (http://mcm.leeds.ac.uk/MCM).

The system of differential equations in the model is integrated with a variable order Gear's method within the FACSIMILE software suite (Curtis and Sweetenham, 1987). The hourly mixing ratios for the majority of NMHC species were input into the model. The acetone formation between the base case and the constrained cases was compared and the major NMHC species that contributed to the acetone formation were identified and quantified.

3. Results and discussion

3.1. General characteristics

3.1.1. Spatial variations

Table 2 presents the main carbonyl compounds at the TMS and TW sites. The carbonyl levels at mountain sites and urban areas in previous studies are also given in the table. Generally, acetone was the most abundant carbonyl compound at both the mountain TMS site and the urban TW site. The acetone concentration at TMS was similar to that at TW ($p = 0.11 > 0.05$), though the TMS site was 630 m higher than the TW site, and farther away from anthropogenic sources, perhaps implying more importance of biogenic sources, and/or photochemical formation, and/or influence of regional transport or mesoscale circulations at the mountain site. Compared to other mountain sites, it was found that the acetone concentration at TMS (640 m a.s.l) was in line with that at Mt. Dinghu (320 m a.s.l.) of inland PRD region, whereas it was much higher than that at Mt. Waliguan (3816 m a.s.l.), China, and Mt. Whiteface (1500 m a.s.l.), USA, reflecting the fact that the PRD region was more polluted. It may also suggest that the acetone level decreased with the increase in height of the sampling sites. Nevertheless, one must bear in mind that the concentrations of an air pollutant are associated with sampling season, sampling duration, sampling location, meteorological conditions, site topography, sampling and analytical methods and so on.

For the urban site (i.e. TW), the mean acetone concentration (9.9 ± 1.4 μg m^{-3}, mean $\pm$ 95% confidence interval) measured in autumn 2010 (i.e. this study) was more than 5 times that (1.8 ± 1.6 μg m^{-3}) in winter 1999/2000, perhaps due to the seasonal variations and/or annual variations in acetone source strength and/or in sources such as vehicular emissions, industrial emissions and secondary formation. Compared to another urban site, the acetone level at TW was similar to that at Tung Chung (TC), whereas the formaldehyde and acetaldehyde levels at TC were much higher than TW, suggesting that the TC site encountered more polluted air. This could be caused by higher local emissions of formaldehyde and

acetaldehyde, and more secondarily formed C$_1$–C$_2$ aldehydes at TC site as it is farther downwind of the inland PRD region and air masses arriving at this site are more aged. It was also found that the acetone concentration at TW was slightly lower than that in Guangzhou, but similar to that in Shanghai and Beijing. However, the levels of formaldehyde and acetaldehyde at TW in Hong Kong were much lower than those in Guangzhou, Shanghai and Beijing.

3.1.2. Temporal variations

i) Day-to-day variations

The day-to-day variations of acetone along with those of O$_3$, CO, isoprene, CH$_3$Cl, i-butane, i-butene, wind speed and wind direction observed at TW and TMS are shown in Fig. 3. The VOC sampling days were characterized by warm and humid weather, with daytime maximum temperature of 24.7–34.4 °C (28.7 $\pm$ 1.5 °C) at TW and 15.8–27.6 °C (21.1 $\pm$ 1.6 °C) at TMS. Precipitation was not observed during the VOC sampling days. The wind speed and wind direction showed large day-to-day variations at the two sites. For instance, at the TMS site, the prevailing winds were northerly. However, the wind speeds were lower in late September and early October, whereas the wind speeds significantly increased on 23–31 October.

Large day-to-day variations were observed for acetone. The mean acetone level during the sampling period was 9.9 μg m^{-3} (1.6–114 μg m^{-3}) at TW and 8.6 μg m^{-3} (1.0–33 μg m^{-3}) at TMS. On some non-O$_3$ episode days i.e. 2, 14 October and 20–21 November, the peak acetone levels at TW were much higher than those at TMS. In contrast, on some O$_3$ episode days such as 23 October, 31 October–2 November, the peak acetone values at TMS were significantly greater than those at TW. However, higher acetone concentrations at TMS were sometimes observed i.e. 8 October, while on some O$_3$ episode days i.e. 3, 9 and 19 November, the acetone levels at TW were greater than at TMS. The highly varied temporal patterns of acetone at both sites suggest that the sources of acetone were complex and multiple. Indeed, by looking into the temporal variations of other air pollutants which are the tracers of potential acetone sources, it was found that acetone had no or weak correlations with O$_3$ ($R^2 = 0.01$ and 0.25 at TW and TMS, respectively), CO ($R^2 = 0.01$ and 0.12), isoprene ($R^2 = 0.03$ and 0.06), CH$_3$Cl ($R^2 = 0.04$ and 0.12), and i-butane ($R^2 = 0.1$ and 0.2). By comparing the temporal variations at the two sites, we also found that the daily concentrations of anthropogenic air pollutants i.e. CO and i-butane were higher at the urban site TW, whereas the daily levels of biomass burning tracer i.e. CH$_3$Cl were similar at the two sites. Opposite to our expectation, the daily biogenic isoprene mixing

Table 2
Comparison with other studies.

Locations	Sampling time	Latitude, longitude	Altitude (m a.s.l.)	HCHO (μg m^{-3})	CH$_3$COCH$_3$ (μg m^{-3})	CH$_3$CHO (μg m^{-3})	Ref[a]
TMS, Hong Kong	Sep.–Nov. 2010	22.405°N, 114.118°E	640	3.3 ± 0.2	8.6 ± 0.7	2.5 ± 0.2	1
Mt. Dinghu, China	Dec. 2006	23.10°N, 112.32°E	320	3.3 ± 3.0	6.6 ± 1.9	3.99 ± 3.5	2
Mt. Waliguan, China	Aug.–Sep. and Dec. 2005	36.28°N, 100.90°E	3816	4.2 ± 1.9/1.5 ± 0.4	2.02 ± 0.86/1.88 ± 0.69	4.25 ± 3.32/3.91 ± 0.81	3
Mt. Whiteface, USA	Jul. 1994	44.37°N, 73.90°W	1500	0.33–1.8	0.89–2.6	0.30–0.78	4
TW, Hong Kong	Sep.–Nov. 2010	22.373°N, 114.112°E	10	3.6 ± 0.2	9.9 ± 1.4	3.9 ± 0.4	1
TW, Hong Kong	Nov.–Feb., 1999–2000	22.373°N, 114.112°E	10	2.6 ± 1.6	1.8 ± 1.6	1.6 ± 0.6	5
TC, Hong Kong	Oct.–Nov. 2007	22.30°N, 113.93°E	0	9.2 ± 2.3	12.4 ± 3.5	8.8 ± 2.0	6
Guangzhou, China	Jun.–Sep. 2003	23.01°N, 113.03°E	0	13.7 ± 2.2	17.8 ± 6.3	8.3 ± 5.1	7
Shanghai, China	Oct. 2007	31.02°N, 121.04°E	0	6.8 ± 1.8	9.6 ± 4.2	8.2 ± 1.9	8
Beijing, China	Sep.–Nov. 2005	39.8°N, 116.5°E	0	15.8 ± 9.7	16.7 ± 7.5	16.2 ± 7.2	9

[a] References: [1] this study, [2] Chi et al. (2008), [3] Mu et al. (2007), [4] Khwaja and Narang (2008), [5] Ho et al. (2002), [6] Guo et al. (2009), [7] Feng et al. (2005), [8] Huang et al. (2008), [9] Pang and Mu (2006).
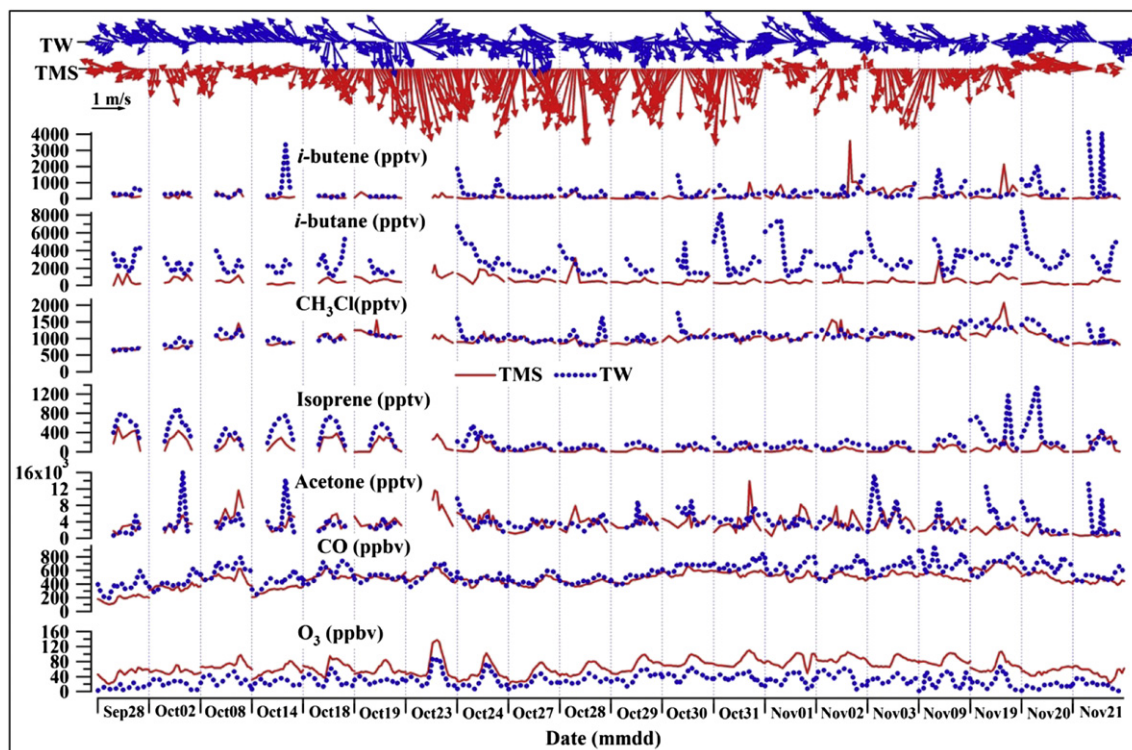
Fig. 3. Time series of O_3, CO, acetone, isoprene, CH_3Cl, *i*-butane, *i*-butene, wind speed and wind direction during the sampling period.

ratios at the mountain site TMS were lower than TW, likely due to the fact that the source strength of biogenic emissions at the two sites were different, and the biogenic emission was closely related to temperature as the temperature at TMS was lower than at TW (Guo et al., 2012).

ii) Diurnal patterns

In order to better understand the potential sources of acetone, the diurnal patterns of acetone at the two sites on O_3 and non-O_3 episode days are presented in Fig. 4. Generally, the mean acetone mixing ratios on O_3 episode days were higher than those on non-O_3 episode day at both sites ($p < 0.05$). It can be seen that on non-O_3 episode days the acetone mixing ratios at TMS showed no difference between daytime (07:00–18:00; 3342 ± 416 pptv) and nighttime ($p = 0.16$; 2409 ± 959 pptv), whereas on O_3 episode days a peak acetone value was observed in late afternoon (16:00), and the daytime mean acetone level (4712 ± 769 pptv) at TMS was significantly greater than the nighttime value (2900 ± 358 pptv; $p < 0.01$),

implying the contribution of photochemical formation and/or biogenic emissions to acetone levels on O_3 episode days at TMS.

On the other hand, the diurnal patterns at TW showed no differences between daytime and nighttime concentrations on O_3 and non-O_3 episode days ($p = 0.92$ and 0.23, respectively). In particular, no obvious acetone peak was found on O_3 episode days at TW, suggesting that there might be primary acetone sources which concealed the acetone peak at noon/in the afternoon produced by photochemical reaction.

The diurnal patterns found at TW on both non-O_3 and O_3 episode days, and at TMS on non-O_3 episode days were consistent with the observation at a coastal marine location in New Hampshire (Mao et al., 2006), and opposite to the findings reported at a continental site in eastern New England (Mao et al., 2006), in the Lower Fraser Valley of British Columbia, Canada (Wang et al., 2005), at downtown Santiago de Chile (Rubio et al., 2006), at a rural site in southern Germany (Slemr et al., 1996), and in urban area of Shanghai, China (Huang et al., 2008). On the other hand, the diurnal variations of acetone at TMS on O_3 episode days were in line with
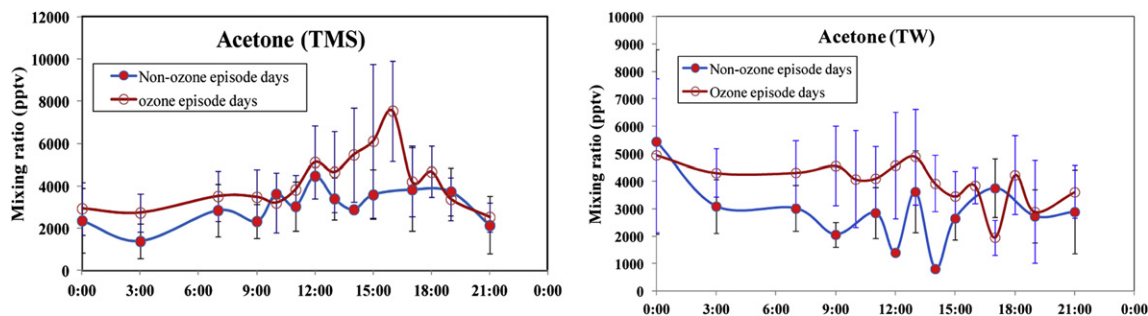

Fig. 4. Mean diurnal patterns of acetone at TMS (left) and TW (right). Error bars represent the spread in measurements in terms of 95 percent confidence interval.

the observations in Canada, Germany and Chile (Slemr et al., 1996; Wang et al., 2005; Rubio et al., 2006), but different from the patterns found in Shanghai (Huang et al., 2008) and in New England (Mao et al., 2006).

3.2. Source apportionment of acetone

As discussed above, the sources of acetone were complex in the studied areas. Hence, it would be instructive if the sources could be identified and quantified. In this study, we applied canister samples into the PMF model for source apportionments. In total, 180 and 201 samples were used for TW and TMS, respectively. As acetone could be emitted from a variety of sources, tracers of different sources were selected for model input. These tracers included CO, ethene and ethyne for combustion, DMS from the ocean, CH_3Cl from biomass burning, C_2Cl_4 for urban sources, isoprene from biogenic emissions, benzene, toluene, ethylbenzene and xylenes from anthropogenic sources such as vehicular emissions and solvent usage, and O_3 for secondary formation via photochemical reactions. Tables 3 and 4 show the PMF extracted source profiles for air samples collected at TW and TMS, respectively. The acetone sources at both sites were similar, namely, biogenic emission, vehicle emission and secondary formation, biomass burning and solvent usage.

The first factor was identified as biogenic emission as the tracer isoprene had the highest concentration in this source for both sites (0.56 and 0.29 μg m^{-3}, respectively).

Elevated concentrations of CO, C_2Cl_4, ethene, ethyne, benzene and toluene were found in the second factor at both sites, suggesting their urban combustion origins i.e. vehicular emissions. The high correlation of C_2Cl_4 with this factor at the urban site, i.e. TW confirmed that this source was urban-related because C_2Cl_4 is primarily used as a dry cleaning solvent and degreasing agent, and the dominance of its anthropogenic production source makes it a useful tracer for urban/industrial activities mixed with urban vehicular emissions (Blake et al., 2003; Simpson et al., 2004; Lai et al., 2010). In addition, the second factor showed high O_3 concentrations for both sites (54.5 and 64.4 μg m^{-3}, respectively), implying the association of secondary formation with the acetone formation. In other words, the second factor was a collocation of vehicular emission and secondary formation. This is not surprising as the tracer for anthropogenic pollution in urban areas i.e. CO is mostly co-emitted with a large number of different hydrocarbons, and is, therefore, related to the secondary production of acetone (de Reus et al., 2003).

Table 3
PMF extracted source profiles for air samples collected at TW (unit: μg m^{-3}).

Species	Biogenic emission	Vehicle emission & secondary formation	Biomass burning	Solvent usage
CO	57.09	163.51	388.54	0.00
DMS	0.02	0.00	0.02	0.01
C_2Cl_4	0.00	0.30	0.15	0.15
CH_3Cl	0.21	0.82	1.06	0.05
Ethene	0.27	0.27	1.48	0.01
Ethyne	0.25	0.81	1.65	0.00
Isoprene	0.56	0.14	0.00	0.05
Benzene	0.01	0.99	1.08	0.22
Toluene	0.19	3.52	1.57	4.61
Ethylbenzene	0.17	0.66	0.00	3.20
m-Xylene	0.22	0.00	0.16	2.46
p-Xylene	0.10	0.13	0.05	1.15
o-Xylene	0.12	0.09	0.06	1.29
Acetone	0.08	5.08	0.89	1.56
O_3	1.38	54.47	1.37	0.00

Table 4
PMF extracted source profiles for air samples collected at TMS (unit: μg m^{-3}).

	Biogenic emission	Vehicle emission & secondary formation	Biomass burning	Solvent usage
CO	42.92	107.20	239.65	6.95
DMS	0.01	0.00	0.00	0.00
C_2Cl_4	0.04	0.09	0.10	0.23
CH_3Cl	0.28	0.53	1.22	0.00
Ethene	0.07	0.14	0.39	0.12
Ethyne	0.11	0.36	0.97	0.17
Isoprene	0.29	0.00	0.00	0.01
Benzene	0.12	0.56	1.02	0.23
Toluene	0.32	0.77	1.24	3.71
Ethylbenzene	0.08	0.19	0.26	1.56
m-Xylene	0.03	0.01	0.13	0.62
p-Xylene	0.02	0.05	0.06	0.43
o-Xylene	0.03	0.05	0.06	0.44
Acetone	0.83	5.82	0.01	1.50
O_3	16.37	64.43	48.12	1.69

The third factor was characterized by high concentrations of CO, CH_3Cl, ethyne, benzene and toluene, consistent with the source profile of biomass burning (Crutzen et al., 1979).

High concentrations of toluene, ethylbenzene, and *m,p,o*-xylenes and very low CO concentrations in factor 4 for both sites clearly indicated that this source was more related to solvent usage in paint (Borbon et al., 2002). The highest C_2Cl_4 concentration among the four factors was also found at the mountain site, i.e. TMS in this factor, suggesting that this source was also associated with drying cleaning and degreasing agent.

By summing up the concentration of acetone in each source, we were able to obtain the total concentration of acetone in the atmosphere (Tables 3 and 4). Hence, the contributions of each individual source to ambient acetone concentrations are computed and presented in Fig. 5. The standard errors in the figure were obtained from bootstrap analyses extracted from PMF results.

It is evident that vehicular emission plus secondary formation ($67 \pm 10\%$) made the most significant contribution to ambient acetone at TW, followed by the use of solvent ($20 \pm 3\%$), biomass burning emissions ($12 \pm 1\%$) and biogenic emission ($1 \pm 2\%$) (Fig. 5a). Similarly, at TMS, the combination of vehicular emission and secondary formation was the largest contributor ($71 \pm 1\%$), while solvent usage made the second highest contribution ($19 \pm 0.1\%$). About $10 \pm 0.2\%$ of the ambient acetone was attributed to biogenic emission whereas the contribution of biomass burning was negligible at the mountain site (Fig. 5b). The results in this study are in contrast to the global budget of acetone obtained by Singh et al. (1994), who used three-dimensional photochemical models to estimate source distributions in the atmosphere. They found that secondary formation from the atmospheric oxidation of precursor hydrocarbons provided the single largest source (51%). The remainder was attributable to biomass burning (26%), direct biogenic emissions (21%), and primary anthropogenic emissions (3%). The receptor modeling results in the present study are also inconsistent with the simulated global source distributions reported by Jacob et al. (2002), who estimated that biogenic emission made the most significant contribution (35%) to acetone, followed by oceanic emissions (28%), atmospheric oxidation of isoalkanes (22%), atmospheric oxidation of monoterpenes (6%), biomass burning (5%), plant decay (2%), atmospheric oxidation of methylbutenol (1%) and anthropogenic emission (solvent use and automobiles; 1%). The inconsistency among the studies suggests high spatial variations of source contributions to acetone.

Although the source contributions of vehicular emission + secondary formation ($67 \pm 10\%$), and solvent usage ($20 \pm 3\%$) at TW were similar to those at TMS, significant differences in source contributions of biomass burning and biogenic emission were
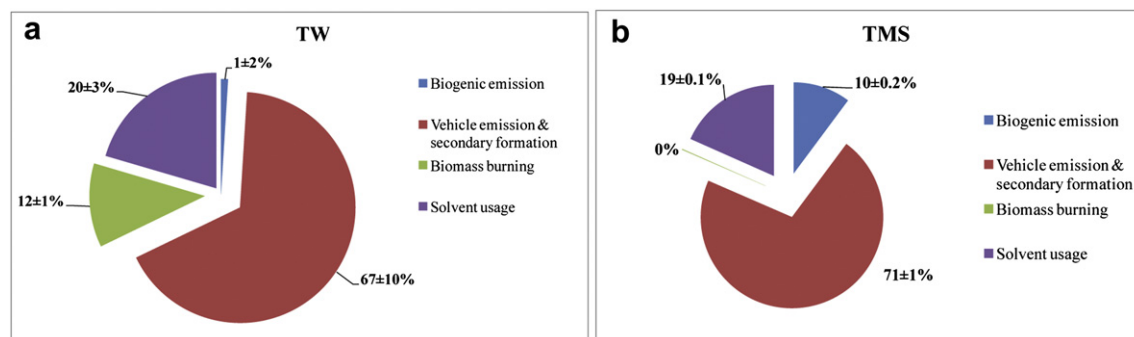
Fig. 5. Source apportionments of acetone at (a) TW and (b) TMS.

observed between the two locations. The contribution of biogenic emission at TMS (i.e. $0.83\ \mu g\ m^{-3}$; $10 \pm 0.2\%$) was about 10 times that from the same source at TW (i.e. $0.08\ \mu g\ m^{-3}$; $1 \pm 2\%$), whereas the contribution from biomass burning at TMS ($0.01\ \mu g\ m^{-3}$; 0.3%) was much lower than that at TW ($0.89\ \mu g\ m^{-3}$; $12 \pm 1\%$) (Tables 3 and 4, Fig. 5). The higher contribution of biogenic emissions at TMS was likely due to the fact that this site was situated at the waist of Mt. TMS ($22.405°$N, $114.118°$E; 640 m a.s.l.), surrounded by dense trees and plants, whereas the urban site, i.e. TW was on the rooftop of a building with a height of 18 m and only tall buildings were around. On the other hand, the greater contribution of biomass burning at TW could be attributable to the barbecue activities at the foot of the mountain as there were several barbecue places for public use and we often witnessed the barbecue activities during the sampling period; and maybe also due to the biomass burning activities at a small village nearby, consistent with our previous study in which biomass burning was identified in Hong Kong (Guo et al., 2011).

3.3. Major mechanism of atmospheric oxidation formation of acetone

In Section 3.2, secondary formation of acetone was identified as the most important source though it could not be separated from vehicular emissions at both sites. Hence, the precursors and their transformation to acetone in the study sites need to be understood. Table 5 shows the results extracted from the photochemical box modeling incorporated with the MCM at TMS and TW.

At TMS, it was found that C_3–C_6 alkanes contributed 28.7% to the secondary formation of acetone, while C_2–C_3 alkenes accounted for 20.0% (Table 5). The contribution of biogenic VOCs

Table 5
Contribution of different VOCs to the formation of acetone during daytime hours (07:00–18:00) extracted from the photochemical box model at TMS and TW.

Scenario	Acetone mixing ratio[a] (ppbv)		Reduction (%)	
	TMS	TW	TMS	TW
Base case	0.66 ± 0.04	1.74 ± 0.11		
Propane constrained	0.61 ± 0.04	1.46 ± 0.08	7.6%	16.1%
i-Butane constrained	0.58 ± 0.04	1.22 ± 0.06	12.0%	29.8%
n-Butane constrained	0.66 ± 0.04	1.78 ± 0.11	0.0%	−2.2%
i-Pentane constrained	0.61 ± 0.04	1.62 ± 0.10	7.6%	6.9%
2-Methylpentane constrained	0.65 ± 0.04	1.71 ± 0.10	1.5%	1.7%
i-Butene constrained	0.53 ± 0.03	1.46 ± 0.09	20.0%	16.1%
i-Pentene constrained	0.66 ± 0.04	1.75 ± 0.11	0.0%	−0.6%
Isoprene constrained	0.66 ± 0.04	1.74 ± 0.11	0.0%	0.0%
α/β-Pinene constrained	0.65 ± 0.04	1.73 ± 0.11	1.5%	0.6%
Limonene constrained	0.66 ± 0.04	1.75 ± 0.11	0.0%	−0.6%

[a] Mean ± 95% confidence interval.

was small (1.5%). The most important contributor to the oxidation formation of acetone was *i*-butene (20%), followed by *i*-butane (12%) and propane and *i*-pentane (7.6%, respectively).

On the other hand, at TW, about 54.5% of the secondarily formed acetone was attributable to C_3–C_6 alkanes, and 16.1% was caused by C_2–C_3 alkenes (Table 5). Again, the biogenic species made negligible contribution to the acetone formation. Nearly 30% of *i*-butane was oxidized by OH radicals to produce acetone, while propane and *i*-butene accounted for 16% of the secondary acetone, respectively.

By comparison, it can be seen that the contribution of C_3–C_6 alkanes to the oxidation formation of acetone at TW was about twice that at TMS, while the fractions for C_2–C_3 alkenes were similar at both sites. Moreover, at the urban TW site the dominant hydrocarbon was a C_4 alkane i.e. *i*-butane, whereas the major contributor at the mountain TMS site was an alkene i.e. *i*-butene.

The results obtained in this study are consistent with what were found by Singh et al. (1994) and Jacob et al. (2002), who suggested that atmospheric oxidation of C_3–C_5 isoalkanes is a major source of acetone. However, the main species responsible for the secondary acetone formation in this study are different from those reported by Singh and Hanst (1981), who claimed that propane was the major precursors of acetone. In this study, *i*-butene and *i*-butane were the most important contributors to the oxidation formation of acetone, despite the elevated contribution of propane at TW.

Propane and *i*/*n*-butanes are mainly emitted from leakage of liquefied petroleum gas (LPG) (Blake and Rowland, 1995), and *i*-butene is the main component of combustion sources (Barletta et al., 2005). In Hong Kong, all taxis and mini-buses are fueled with LPG, and other vehicles use gasoline and/or diesel as fuel. Thus, the oxidation formation of acetone in Hong Kong would be remediated by controlling the leakage of LPG and emissions of vehicular exhaust.

In the previous section, the source apportionment of acetone could not separate the contribution of vehicular emissions from the secondary formation of acetone. However, since the mixing ratios of secondarily formed acetone at both sites were obtained from the photochemical box modeling, the source apportionment results in Fig. 4 could be further refined. At TMS, the secondary acetone concentration was $1.56\ \mu g\ m^{-3}$ (0.66 ppbv in Table 5), and the contribution of vehicular emission and secondary formation was $5.82\ \mu g\ m^{-3}$ (Table 4). As such, the contribution of secondary sources to acetone at TMS was ($71\% \times 1.56/5.82$) = 19%; and the vehicular emission was 52%. Similarly, at TW, the secondary acetone level was $4.11\ \mu g\ m^{-3}$ (1.74 ppbv in Table 5), and the total contribution of vehicular emission and secondary formation was $5.08\ \mu g\ m^{-3}$ (Table 3). Therefore, secondary sources made 54% contribution to the ambient acetone; and vehicular emission being 13%. The refined results clearly indicated that vehicular emission made the most significant contribution (52%) to ambient acetone at the mountain

site (i.e. TMS) whereas the major contributor to ambient acetone at the urban site (i.e. TW) was the secondary sources (54%).

4. Conclusions

In this study, field measurements were simultaneously carried out at different elevations on the highest mountain in Hong Kong, Mt. Tai Mo Shan, from 06 September to 29 November, 2010. Analysis of spatiotemporal patterns indicated that the acetone concentration was similar at both sites, and the mean acetone mixing ratios on O_3 episode days were higher than those on non-O_3 episode day on both sites ($p < 0.05$).

Receptor modeling results showed that vehicular emission plus secondary formation made the most significant contribution to ambient acetone at the two sites, followed by the use of solvent. At the mountain site, biogenic emission was the third largest contributor to ambient acetone while it was negligible at the urban site. In contrast, biomass burning made 12% contribution to ambient acetone at the urban site and very minor contribution at the mountain site.

Simulation of the photochemical box model found that the precursors of secondary acetone in this study were C_3–C_6 alkanes and C_2 alkene. At the mountain site, *i*-butene was the most important precursor of ambient acetone, followed by *i*-butane. At the urban site, *i*-butane, propane and *i*-butene were the most important precursors of acetone. The contribution of biogenic VOCs was negligible.

Acknowledgments

References

Arnold, F.A., Schneider, J., Gollinger, K., Schlager, H., Schulte, P., Hagen, D.E., Whitefield, P.D., van Velthoven, P., 1997. Observation of upper tropospheric sulfur dioxide and acetone pollution: potential implications for hydroxyl radical and aerosol formation. Geophysical Research Letters 24, 57–60.

Barletta, B., Meinardi, S., Rowland, F.S., Chan, C.-Y., Wang, X.M., Zou, S.C., Chan, L.Y., Blake, D.R., 2005. Volatile organic compounds in 43 Chinese cities. Atmospheric Environment 39, 5979–5990.

Blake, D.R., Rowland, F.S., 1995. Urban leakage of liquefied petroleum gas and its impact on Mexico City air quality. Science 269, 953–956.

Blake, N., et al., 2003. NMHCs and halocarbons in Asian continental outflow during the Transport and Chemical Evolution over the Pacific (TRACE-P) Field Campaign: comparison with PEM-West B. Journal of Geophysical Research 108 (D20), 8806. http://dx.doi.org/10.1029/2002JD003367.

Borbon, A., Locoge, N., Veillerot, M., Galloo, J.C., Guilermo, R., 2002. Characterization of NMHCs in a French urban atmosphere: overview of the main sources. Science of the Total Environment 292, 177–191.

Chi, Y.G., Li, Z.Y., Feng, Y.L., Wen, S., Yu, Z.Q., Sheng, G.Y., Fu, J.M., 2008. Carbonyl compound concentrations in the air at Dinghu Mountain, Guangdong Province. Acta Scientiae Circumstantiae 28 (11), 2347–2353.

Colman, J.J., Swanson, A., Meinardi, S., Sive, B.C., Blake, D.R., Rowland, F.S., 2001. Description of the analysis of a wide range of volatile organic compounds in whole air samples collected during PEM-tropics A and B. Journal of Analytical Chemistry 73, 3723–3731.

Crutzen, P.J., Heidt, L.E., Krasnec, J.P., Pollock, W.H., Seiler, W., 1979. Biomass burning as a source of atmospheric gases CO, H_2, N_2O, NO, CH_3Cl and COS. Nature 282 (5736), 253–256.

Curtis, A.R., Sweetenham, W.P., 1987. FACSIMILE Release H User's Manual. AERE Report R11771 (HMSO), London.

de Laat, A.T.J., de Gouw, J.A., Lelieveld, J., 2001. Model analysis of trace gas measurements and pollution impact during INDOEX. Journal of Geophysical Research 106 (D22), 28469–28480.

de Reus, M., Fischer, H., Arnold, F., de Gouw, J., Holzinger, R., Warneke, C., Williams, J., 2003. On the relationship between acetone and carbon monoxide in different air masses. Atmospheric Chemistry and Physics 3, 1709–1723.

Eerdekens, G., Ganzeveld, L., Vilà-Guerau de Arellano, J., Klüpfel, T., Sinha, V., Yassaa, N., Williams, J., Harder, H., Kubistin, D., Martinez, M., Lelieveld, J., 2009. Flux estimates of isoprene, methanol and acetone from airborne PTR-MS measurements over the tropical rainforest during the GABRIEL 2005 campaign. Atmospheric Chemistry and Physics 9, 4207–4227.

Elias, T., Szopa, S., Zahn, A., Schuck, T., Brenninkmeijer, C., Sprung, D., Slemr, F., 2011. Acetone variability in the upper troposphere: analysis of CARIBIC observations and LMDz-INCA chemistry-climate model simulations. Atmospheric Chemistry and Physics 11, 8053–8074.

Feng, Y., Wen, S., Chen, Y., Wang, X., Lü, H., Bi, X., Sheng, G., Fu, J., 2005. Ambient levels of carbonyl compounds and their sources in Guangzhou, China. Atmospheric Environment 39, 1789–1800.

Fischer, E.V., Jacob, D.J., Millet, D.B., Yantosca, R.M., Mao, J., 2012. The role of the ocean in the global atmospheric budget of acetone. Geophysical Research Letters 39, L01897. http://dx.doi.org/10.1029/2011GL050086.

Floberth, G.A., Hauglustaine, D.A., Lathière, J., Brocheton, F., 2006. Interactive chemistry in the Laboratoire de Météorologie Dynamique general circulation model: model description and impact analysis of biogenic hydrocarbons on tropospheric chemistry. Atmospheric Chemistry and Physics 6, 2273–2319. http://dx.doi.org/10.5194/acp-6-2273-2006.

Gierczak, T., Burkholder, J.B., Bauerle, S., Ravishankara, A.R., 1998. Photochemistry of acetone under tropospheric conditions. Chemical Physics 231, 229–244.

Goldstein, A.H., Schade, G.W., 2000. Quantifying biogenic and anthropogenic contributions to acetone mixing ratios in a rural environment. Atmospheric Environment 34, 4997–5006.

Guo, H., Lee, S.C., Louie, P.K.K., Ho, K.F., 2004. Characterization of hydrocarbons, halocarbons and carbonyls in the atmosphere of Hong Kong. Chemosphere 57, 1363–1372.

Guo, H., Jiang, F., Cheng, H.R., Simpson, I.J., Wang, X.M., Ding, A.J., Wang, T.J., Saunders, S.M., Wang, T., Lam, S.H.M., Blake, D.R., Zhang, Y.L., Xie, M., 2009. Concurrent observations of air pollutants at two sites in the Pearl River Delta and the implication of regional transport. Atmospheric Chemistry and Physics 9, 7343–7360.

Guo, H., Cheng, H.R., Ling, Z.H., Louie, P.K.K., Godwin, A.G., 2011. Which emission sources are responsible for the volatile organic compounds in the atmosphere of Pearl River Delta? Journal of Hazardous Materials 188, 116–124.

Guo, H., Ling, Z.H., Simpson, I.J., Blake, D.R., Wang, D.W., 2012. Observations of isoprene, methacrolein (MAC) and methyl vinyl ketone (MVK) at a mountain site in Hong Kong. Journal of Geophysical Research 117, D19303. http://dx.doi.org/10.1029/2012JD017750.

HKCSD (Hong Kong Census and Statistics Department), 2010. Projections of Population Distribution. http://www.statistics.gov.hk/publication/.

Ho, K.F., Lee, S.C., Louie, P.K.K., 2002. Seasonal variation of carbonyl compound concentrations in urban area of Hong Kong. Atmospheric Environment 36 (8), 1259–1265.

Huang, J., Feng, Y., Li, J., Xiong, B., Feng, J., Wen, S., Sheng, G., Fu, J., Wu, M., 2008. Characteristics of carbonyl compounds in ambient air of Shanghai, China. Journal of Atmospheric Chemistry 61, 1–20.

Jacob, S.J., Field, B.D., Jin, E.M., Bey, I., Li, Q., Logan, J.A., Yantosca, R.M., 2002. Atmospheric budget of acetone. Journal of Geophysical Research 107 (D10). http://dx.doi.org/10.1029/2001JD000694.

Jenkin, M.E., Saunders, S.M., Pilling, M.J., 1997. The tropospheric degradation of volatile organic compounds: a protocol for mechanism development. Atmospheric Environment 31, 81–104.

Khwaja, H.A., Narang, A., 2008. Carbonyls and non-methane hydrocarbons at a rural mountain site in northeastern United States. Chemosphere 71, 2030–2043.

Lai, S.C., Baker, A.K., Schuck, T.J., van Velthoven, P., Oram, D.E., Zahn, A., Hermann, M., Weigelt, A., Slemr, F., Brenninkmeijer, C.A.M., Ziereis, H., 2010. Pollution events observed during CARIBIC flights in the upper troposphere between South China and the Philippines. Atmospheric Chemistry and Physics 10, 1649–1660.

Lai, S.C., Baker, A.K., Schuck, T.J., Slemr, F., Brenninkmeijer, C.A.M., van Velthoven, P., Oram, D.E., Zahn, A., Ziereis, H., 2011. Characterization and source regions of 51 high-CO events observed during Civil Aircraft for the Regular Investigation of the Atmosphere Based on an Instrument Container (CARIBIC) flights between south China and the Philippines, 2005–2008. Journal of Geophysical Research 116, D20308. http://dx.doi.org/10.1029/2011JD016375.

Legreid, G., Folini, D., Staehelin, J., Balzani Lööv, J., Steinbacher, M., Reimann, S., 2008. Measurements of organic trace gases including oxygenated volatile organic compounds at the high alpine site Jungfraujoch (Switzerland): seasonal variation and source allocations. Journal of Geophysical Research 113, D05307. http://dx.doi.org/10.1029/2007JD008653.

Mao, H., Talbot, R., Nielsen, C., Sive, B., 2006. Control on methanol and acetone in marine and continental atmospheres. Geophysical Research Letters 33, L02803. http://dx.doi.org/10.1029/2005GL024810.

Mu, Y., Pang, X., Quan, J., Zhang, X., 2007. Atmospheric carbonyl compounds in Chinese background area: a remote mountain of the Qinghai-Tibetan Plateau. Journal of Geophysical Research 112, D22302. http://dx.doi.org/10.1029/2006JD008211.

Paatero, P., 1997. Least squares formation of robust non-negative factor analysis. Chemometrics Intelligent Laboratory Systems 37, 23–35.

Pang, X., Mu, Y., 2006. Seasonal and diurnal variations of carbonyl compounds in Beijing ambient air. Atmospheric Environment 40, 6313–6320.

Rubio, M.A., Zamorano, N., Lissi, E., Rojas, A., Gutiérrez, L., von Baer, D., 2006. Volatile carbonylic compounds in downtown Santiago, Chile. Chemosphere 62, 1011–1020.

Simpson, I.J., Meinardi, S., Blake, N.J., Rowland, F.S., Blake, D.R., 2004. Long-term decrease in the global atmospheric burden of tetrachloroethene (C_2Cl_4). Geophysical Research Letters 31, L08108. http://dx.doi.org/10.1029/2003GL019351.

Simpson, I.J., Blake, N.J., Barletta, B., Diskin, G.S., Fuelberg, H.E., Gorham, K., Huey, L.G., Meinardi, S., Rowland, F.S., Vay, S.A., Weinheimer, A.J., Yang, M., Blake, D.R., 2010. Characterization of trace gases measured over Alberta oil sands mining operations: 76 speciated C_2–C_{10} volatile organic compounds (VOCs), CO_2, CH_4, CO, NO, NO_2, NO_y, O_3 and SO_2. Atmospheric Chemistry and Physics 10, 11931–11954. http://dx.doi.org/10.5194/acp-10-11931-2010.

Singh, H.B., Hanst, P.L., 1981. Peroxyacetyl nitrate (PAN) in the unpolluted atmosphere: an important reservoir for nitrogen oxides. Geophysical Research Letters 8, 941–944.

Singh, H.B., Hara, O.', Herlth, D., Sachse, W., Blake, D.R., Bradshaw, J.D., Kanakidou, M., Crutzen, P.J., 1994. Acetone in the atmosphere: distribution, sources, and sinks. Journal of Geophysical Research 99 (D1), 1805–1819.

Singh, H.B., et al., 2004. Analysis of the atmospheric distribution, sources, and sinks of oxygenated volatile organic chemicals based on measurements over the Pacific during TRACE-P. Journal of Geophysical Research – Atmospheres 109, D15S07. http://dx.doi.org/10.1029/2003JD003883.

Slemr, J., Junkermann, W., Volz-Thomas, A., 1996. Temporal variations in formaldehyde, acetaldehyde and acetone and budget of formaldehyde at a rural site in southern Germany. Atmospheric Environment 30 (21), 3667–3676.

Solberg, S., Dye, C., Schmidbauer, N., Herzog, A., Gehrig, R., 1996. Carbonyls and nonmethane hydrocarbons at rural European sites from the Mediterranean to the Arctic. Journal of Atmospheric Chemistry 25, 33–66.

Sprung, D., Zahn, A., 2010. Acetone in the upper troposphere/lowermost stratosphere measured by the CARIBIC passenger aircraft: distribution, seasonal cycle, and variability. Journal of Geophysical Research 115, D16301. http://dx.doi.org/10.1029/2009JD012099.

Taddei, S., Toscano, P., Gioli, B., Matese, A., Miglietta, F., Vaccari, F.P., Zaldei, A., Custer, T., Williams, J., 2009. Carbon dioxide and acetone air-sea fluxes over the southern Atlantic. Environmental Science and Technology 43, 5218–5222.

Wang, D., Fuentes, J.D., Travers, D., Dann, T., Connolly, T., 2005. Non-methane hydrocarbons and carbonyls in the Lower Fraser Valley during PACIFIC 2001. Atmospheric Environment 39, 5261–5272.

Williams, J., Holzinger, R., Gros, V., Xu, X., Altas, E., Wallace, D.W.R., 2004. Measurements of organic species in air and seawater from the tropical Atlantic. Geophysical Research Letters 31 (23), L23S06.